ISBN: 978-3-95450-216-5 doi:10.18429/JACoW-eeFACT2018-WEYAA03

# SRF SYSTEMS FOR KEKB AND SuperKEKB

K. Nakanishi, M. Nishiwaki#, T. Kobayashi, KEK, Tsukuba, Japan
K. Hirosawa, SOKENDAI, Tsukuba, Japan

*Abstract*

Eight superconducting accelerating cavities were operated for more than ten years at the KEKB. Commisioning operation of SuperKEKB is ongoing and those cavities are also used to accelerate the electron beam of 2.6 A. There are some issues to address the large beam current and to realize stable operation. One issue is a large HOM power of 37 kW expected to be induced in each cavity module. In particular, the power emitted out to the downstream of the cavity is simulated to be large. To cope with the HOM power issue, we have installed an additional HOM damper to the downstream of the cavity module. Another issue is degradation of Q values of the cavities during the ten years operation. Cause of the degradation was particle contamination. To clean the cavity surface, high pressure rinsing (HPR) is an effective way. Therefore we have developed a horizontal HPR. In this method, a nozzle for water jet is inserted horizontally into the cavity module without disassembly of the cavity. We applied the horizontal HPR to our degraded cavities. The RF performances of those cavities have been successfully recovered. In this report, present status of our cavity will be presented. Additionally, low level RF control issues for SuperKEKB upgrade will be introduced.

Table 1: RF-related Operation Parameters in HER

| Parameters | KEKB (operation) | SuperKEKB (design) |
|---|---|---|
| Energy [GeV] | 8.0 | 7.0 |
| Beam current [A] | 1.4 | 2.6 |
| Number of bunches | 1585 | 2500 |
| Bunch length [mm] | 6~7 | 5 |
| Total beam power [MW] | ~5 | 8.0 |
| Total RF voltage [MV] | 15.0 | 15.8 |

## OVERVIEW OF KEKB AND SUPERCONDUCTING CAVITY

KEKB accelerator was an electron-positron asymmetric energy ring collider for B-meson physics, consisting of high energy ring (HER) for the electrons and low energy ring (LER) for the positrons. The circumference was around 3 km. The beam energies of HER and LER were 8 and 3.5 GeV, respectively. The maximum beam currents were 1.4 A for HER and 2.0 A for LER. KEKB was operated until June 2010, with a world record luminosity of $2.1\times10^{34}$ /cm$^2$/s [1].

One serious concern for high-current storage rings is the coupled-bunch instability caused by the accelerating mode of the cavities. This issue arises from the large detuning of the resonant frequency of the cavities that is needed to compensate for the reactive component of the beam loading. In order to mitigate this problem, two types of cavities ware adopted in KEKB operation [2, 3]: one is a superconducting cavity (SCC) [4, 5], and the other is a normal conducting cavity called ARES [6, 7]. ARES, which is a unique cavity specialized for KEKB, consists of a three-cavity system operated in the $\pi/2$ mode: the accelerating (A-) cavity is coupled to a storage (S-) cavity via a coupling (C-) cavity. The A-cavity has higher-order-modes (HOM) damped structures.

In HER, RF systems consisted of hybrid system of eight superconducting cavities (SCC, Fig. 1) and 12 ARES cavities, while LER was operated with 20 ARES cavities without SCCs. Table 1 shows operation-related parameters of HER. The total beam power was 5 MW and the total RF voltage was 15 MV. The large beam power and RF voltage were shared with SCC and ARES cavities by giving an appropriate beam phase-offset between them so that each SCC delivered the power of 400 kW to the beam. The HOM load induced by the large beam current was absorbed by a set of ferrite HOM dampers located at the beam pipes of both ends of the cavity, called small beam pipe (SBP) and large beam pipe (LBP). The absorbed power in 1.4 A-operation reached 16 kW without any problems.

Operation statistics and maintenances of SCC in KEKB were summarized in Ref. [3] in detail. Many monitors were set over the ring to identify a cause of each trip. RF trips of the SCC were mainly caused by discharging in the cavity or a high power input coupler. The trip rate in eight cavities was 0.5 times/day at 1.4 A-operation. After adopting the crab crossing, the trip rate decreased to 0.1 times/day because the beam current was lowered to 1.1 A. In order to maintain stable operations, 1) warming up the system to room temperature was performed twice a year, 2) safety inspections due to high pressure safety regulations of cryogenics were carried out once a year, 3) the input coupler conditioning before cooling with bias voltage was performed and 4) regular conditioning every 2 or 3 weeks was carried out. As a result, SRF system of KEKB had been operated safely and stably.

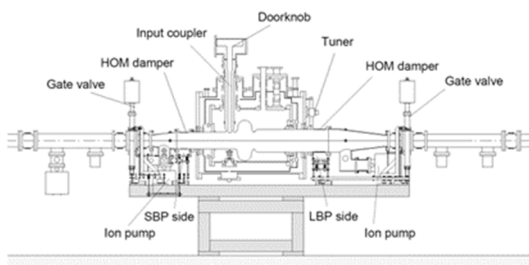


Figure 1: Cross-sectional drawing of the superconducting cavity module of KEKB.

#michiru.nishiwaki@kek.jp

ISBN: 978-3-95450-216-5 doi:10.18429/JACoW-eeFACT2018-WEYAA03

Table 2: SCC Parameters

| Parameters | KEKB (operation) | SuperKEKB (design) |
|---|---|---|
| Number of cavities | 8 | 8 |
| Beam current [A] | 1.4 | 2.6 |
| Bunch length [mm] | 6 | 5 |
| RF voltage [MV/cav.] | 1.5 | 1.5 |
| Beam power [kW/cav.] | 400 | 400 |
| External Q | $5\times10^4$ | $5\times10^4$ |
| Unloaded Q at 1.5 MV | $1\times10^9$ | $1\times10^9$ |
| HOM power [kW/cav.] | 16 | 37 |

## ISSUES OF SCC FOR UPGRADE TO SUPERKEKB

SuperKEKB is an upgrade machine from KEKB to search for "new physics" beyond the Standard Model. The design luminosity is $8\times10^{35}$ /cm$^2$/s, which is 40 times higher than that of KEKB [8]. To achieve high luminosity, the design of SuperKEKB is based on a nano-beam scheme. In the scheme, a vertical beam size at an interaction point is designed as 40-50 nm. At the same time, the beam currents will be twice higher than those of KEKB. The first commissioning operation (Phase-1) was performed from Feb. to June 2016 without beam collision. After the installation of Belle-II detector and the positron damping ring commissioning, the second commissioning (Phase-2) was operated successfully from Mar. to July 2018 including the beam collision tuning [9-11].

The design parameters related with RF system of HER are listed in Table 1. The values of KEKB are achieved values [12]. Basically, existing SRF system including cryogenics are to be re-used in order to minimize the modification for SuperKEKB. The main issues are the higher beam current, the shorter bunch length and the large beam power. The beam power will be shared with SCC and ARES as in the case of KEKB. Therefore the beam power delivered by SCC does not change. The SCC-related parameters for KEKB and SuperKEKB are shown in Table 2. The RF voltage is also the same as KEKB. On the other hand, the HOM power becomes large. The expected power reaches 37 kW due to the high beam currents and shorter bunch length. Therefore, the power capacity of existing HOM dampers could be a serious problem.

Additionally, some cavities have been degraded with field emission. Although the degradation is acceptable in SuperKEKB operation, we will need to recover the cavity performance, if the cavities get more degradation. In that case, we have to spend a long time and huge cost to recover the cavity by conventional way. In order to recover efficiently, we need to consider new technique for the performance recovery of the cavities.

We will report a new calculation method to study the SiC damper as countermeasures for the large HOM power and development of new high pressure rinsing system to recover the performances of the degraded cavities.

Figure 2: A KEKB type LBP damper with 4-mm thickness of ferrite, ϕ300 mm, length of 150 mm.

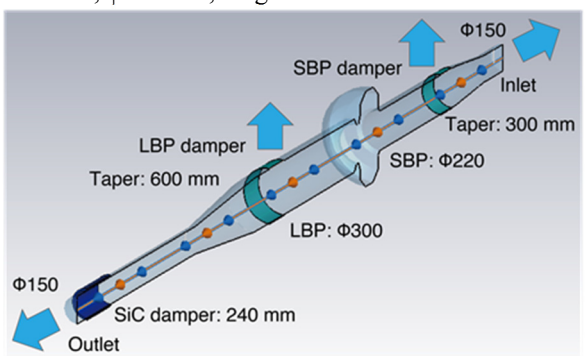


Figure 3: Calculation model of the SCC module. Bunched beam comes from Pin side. Monitors are set at SBP and LBP ferrite dampers and both ends of beam pipes.

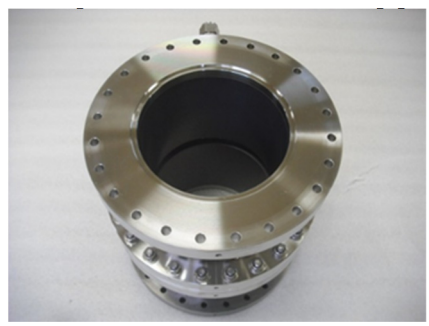

Figure 4: A prototype SiC damper of 240 mm in total length. Two 120-mm SiC dampers are connected together. The thickness of SiC is 10 mm and the inner diameter is 150 mm. The duct length is 220 mm with flanges. The dampers are equipped with a jacket-type water cooling channel.

## MEASURES AGAINST HOM POWER

Figure 2 shows a KEKB type ferrite HOM damper. The ferrite was sintered on the copper base pipe by the hot isostatic press (HIP) method. The thickness of the ferrite was chosen as 4 mm for the optimum HOM damping [13]. A pair of the dampers is installed to SBP and LBP. To estimate the HOM load distribution in the module, we developed a new calculation method using CST Particle Studio: wakefield solver [14]. Wake field power flow monitors are set at the surface of dampers and the end of beam pipes as shown in Fig. 3. The time integrals of the power flow signals over the surface give emitted and

ISBN: 978-3-95450-216-5 doi:10.18429/JACoW-eeFACT2018-WEYAA03



absorbed energies through the beam pipe or in the dampers. The total energy including stored energy in the cavity structure is consistent with the energy deposit independently calculated from the loss factor. Using the ratio of the energy, we can get equivalent loss factors and HOM loads of each component as shown in Table 3.

From the calculation results, the existing SBP and LBP ferrite damper loads are not large. However the emitted out power through the outlet beam pipe toward the downstream cavity becomes large. Therefore, the large emission power should be managed.

To reduce the emission power, we studied an additional silicon carbide (SiC) damper using the same calculation method. The SiC damper was located at downstream of outlet beam pipe. From calculation of the loss factor, the length of the damper was optimized to be 240 mm for our SCC modules. The emission power can be 70% reduced by 240-mm SiC damper as shown in Table 3. The loads of ferrite dampers do not change significantly. We will adopt the additional SiC damper as the first measure against the large HOM power [15].

The additional SiC dampers can be installed to the beam pipe outside the gate valve of the module. Therefore, the performance degradation risk due to the air exposure of cavity surface can be avoided.

Table 3: Summary of Equivalent Loss Factors (Eq. LF) and HOM Loads at 2.6-A Beam Operation

| Part | Without SiC | | With 240-mm SiC | |
|---|---|---|---|---|
| | Eq.LF [V/pC] | HOM Load [kW] | Eq.LF [V/pC] | HOM Load [kW] |
| Inlet | 0.05 | 1.3 | 0.05 | 1.4 |
| Outlet | 0.57 | 15.4 | 0.15 | 4.0 |
| SBP damper | 0.32 | 8.7 | 0.35 | 9.5 |
| LBP damper | 0.44 | 11.8 | 0.47 | 12.8 |
| Total | 1.38 | 37.2 | 1.02 | 27.7 |
| SiC damper | - | - | 0.97 | 26.1 |

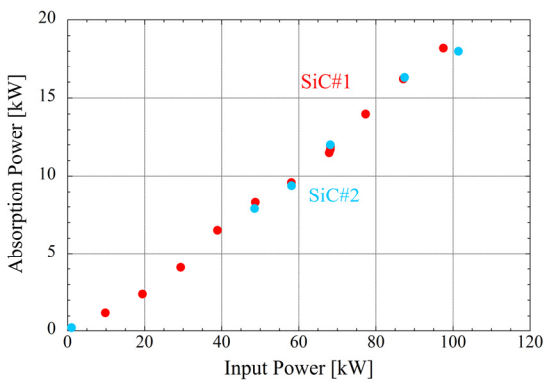


Figure 5: High power RF test results of the prototype of SiC dampers. The absorption powers of 18 kW were achieved by both dampers under the water flow rate of 15 L/min.

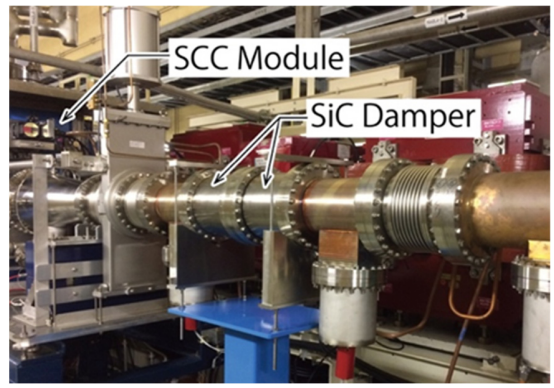


Figure 6: The prototype SiC damper with beam ducts installed downstream of one SCC module. Total SiC length is 240 mm.

A prototype SiC damper consist of two 120-mm SiC dampers (Fig. 4) was fabricated based on the above results. Figure 5 shows the results of the high power absorption tests of the dampers with 15 L/min of the flow late of cooling water. In the tests, the absorption power reached 18 kW for both dampers. The total absorbed power is 1.3 times higher than that of calculation results. The surface temperature of SiC in 18-kW absorption was 80 degrees C and there were no cracks of the surface by the microscope observation after the high power tests.

The prototype SiC damper has been installed before Phase-2 operation (Fig. 6). In Phase-2 operation, the beam test of the SiC damper was performed. Figure 7 shows the absorbed power by the ferrite dampers of the cavities at the beam current of around 760 mA in Phase-1 and Phase-2 operation. The absorbed power of D10B cavity that is downstream of SiC damper decreased remarkably in Phase-2 operation. It was confirmed that the additional SiC damper is effective to reduce the emission power to the downstream cavity.

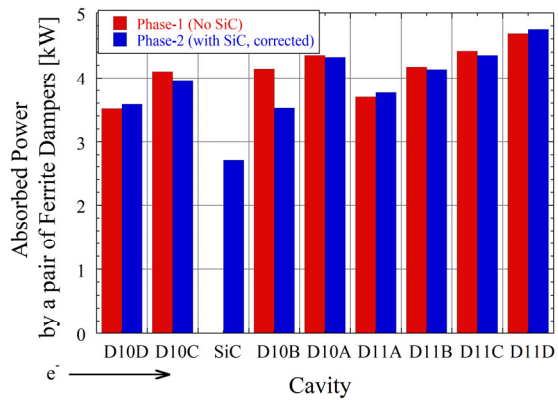


Figure 7: Absorbed HOM power by a pair of ferrite dampers of each cavity. Red: Phase-1 (No SiC damper), Blue: Phase-2 (with SiC damper, with correction factor of 1.05 to correct the systematic error). D10D, D10C and etc on horizontal axis are the cavity name. The beam operation conditions were almost same, the current was around 760 mA. The beam direction is from left to right of the plot. The HOM power of D10B was remarkably decreased by the SiC damper at downstream of D10C in Phase-2 operation.

ISBN: 978-3-95450-216-5 doi:10.18429/JACoW-eeFACT2018-WEYAA03

The SiC dampers will be installed to the other cavities to cope with the large beam current operation.

## PERFORMANCE RECOVERY OF DEGRADED CAVITIES

In the long term operation in KEKB, degradation of the SCC performance was observed. The Q values of several cavities degraded significantly at 2 MV with field emission. The degradation of the cavities was caused by the particle contamination during repair work of vacuum leak and change work of coupler gaskets. In the design of SuperKEKB, the present degradations are acceptable because the required RF voltage is 1.5 MV. However further degradation makes the operation difficult. Therefore performance recovery is desirable for stable and long term operation.

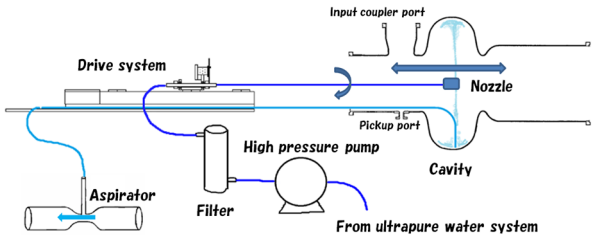


Figure 8: Schematic view of Horizontal HPR system.

Table 4: Horizontal HPR Parameters

| | |
|---|---|
| Water pressure | 7 MPa |
| Nozzle | Martensitic stainless steel, ϕ0.54 mm in dia., 6 holes |
| Driving speed | 1 mm/sec. |
| Rotation speed | 6 degrees/sec. |
| Rinsing time | 15 min. |

### *Development of Horizontal High Pressure Rinse*

High pressure rinse (HPR) is well known as an effective method to clean up the cavity surface contaminants. If it is possible to apply the HPR to the degraded cavity in the cryomodule, we can omit the re-assembling process, and reduce the risk of contaminations and accidents in the re-assembling process. Furthermore, we can save the time and the cost.

New horizontal HPR (HHPR) system with ultra-pure water (18.2 MΩ cm) was developed to apply HPR to the degraded cavity [16]. The schematic view of HHPR system is shown in Fig. 8. The system can be set to the cavity without disassembling the cryomodule. Outside accessories such as an inner conductor of input coupler and both end groups including ferrite HOM dampers, bellows chambers, vacuum system and gate valves are dismounted in a clean booth before HHPR. In the system, the water jet nozzle is inserted to the cavity horizontally (Fig. 9). The nozzle is driven automatically in horizontal and rotational movements. Collected water in the cell is pumped up by an aspiration system during rinsing. The HHPR parameters are summarized in Table 4. The HHPR and vertical tests had been performed to the prototype cavity. In the test, the degraded $Q_0$ of the cavity was recovered successfully without baking after HHPR [16].

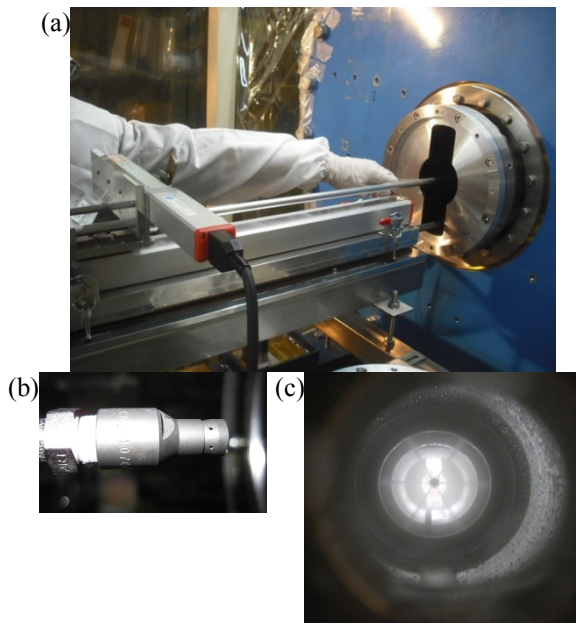


Figure 9: HHPR apparatus. (a) Stainless steel pipe with nozzle inserted from SBP side, (b) nozzle head with 6 holes, (c) water jets during rinsing.

### *HHPR to Degraded Cavities and Q-Measurements*

The HHPR applied to three degraded cavities. The cavities were dried up by evacuation for 4 days before setting the input coupler, the HOM dampers and vacuum system. After setting, the cavities were evacuated by a tarbo-moleculer pump and then switched to ion pumps. The baking was not given in the same way as the prototype cavity.

Before cooling down the cavity, the input coupler was conditioned with high RF power up to 300 kW so as to process the electron multipacting discharge on the coupler and outer conductor surfaces. DC bias voltage up to ±2 kV was applied to the inner conductor [17]. Since the outer conductor surface was exposed to the HHPR water, much water molecules adsorb on the surface even after dried up sufficiently. The minus voltage bias that enhances the multipacting discharge on the outer conductor surface was more effective to condition.

ISBN: 978-3-95450-216-5 doi:10.18429/JACoW-eeFACT2018-WEYAA03



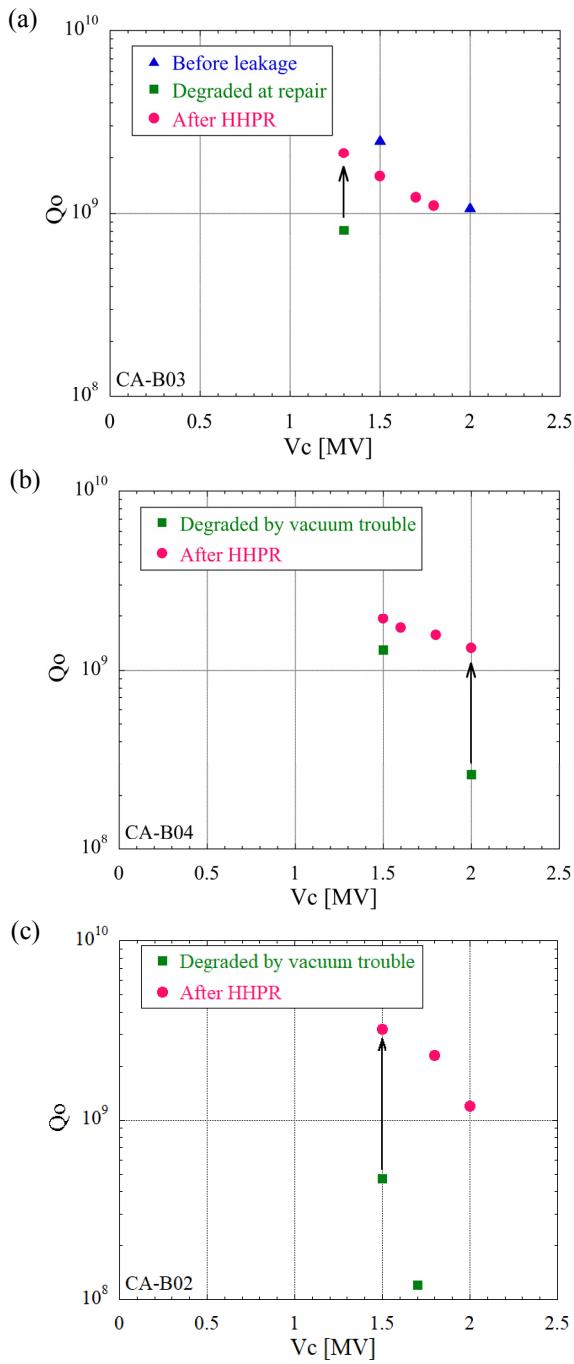


Figure 10: $Q_0$ measurement results of degraded cavities after HHPR. (a) CA-B03 was degraded at repair work. (b) CA-B04 and CA-B02 were degraded by vacuum trouble. The $Q_0$ values of all cavities were recovered successfully.

The cavity modules were cooled down to 4.4 K. And then high power conditioning started. Figure 10 show results of the high power test of two cavities. The $Q_0$ values at each cavity voltage were obtained from the helium consumption rate of the cryomodule. Degraded cavity "CA-B03" (Fig. 10 (a)) had a leak at indium sealed joint of the beam pipe. The cavity module was disassembled and repaired the leak. But the $Q_0$ values significantly degraded with strong field emission. In the high power test after HHPR, the field emission of the cavity was significantly improved. The cavity voltage was finally achieved 2 MV. The field was limited by the radiation safety in the test stand. The $Q_0$ value is acceptable for SuperKEKB operation. Cavities "CA-B04" and "CA-B02" had vacuum troubles 10 years ago (Fig. 10 (b)) and before Phase-1 operation (Fig. 10 (c)), respectively. Some amount of air dust was accidentally introduced to the cavities and $Q_0$ values degraded with strong field emission. After this HHPR, the $Q_0$ values at 2 MV of the cavities increased above $1\times10^9$ with less field emission. Three cavity performances were successfully recovered by the HHPR. Two of these modules were installed to the ring for SuperKEKB operation. Another one is reserved as a spare cavity module.

## RF CONTROL ISSUES FOR SUPERKEKB

### *Low Level RF Control System*

Accuracy and flexibility in accelerating field control are very essential for high-current storage and high-quality beam without instability. Therefore, new low-level RF (LLRF) control system, which is based on recent digital architecture, was developed for the SuperKEKB upgrade [18]. Figure 11 shows a picture of a mass-

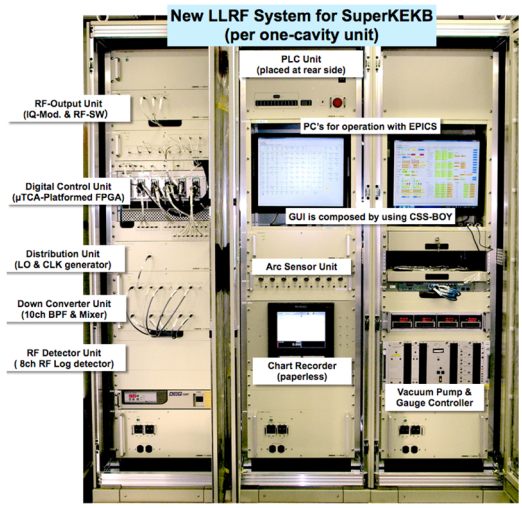


Figure 11: New LLRF control system for SuperKEKB.

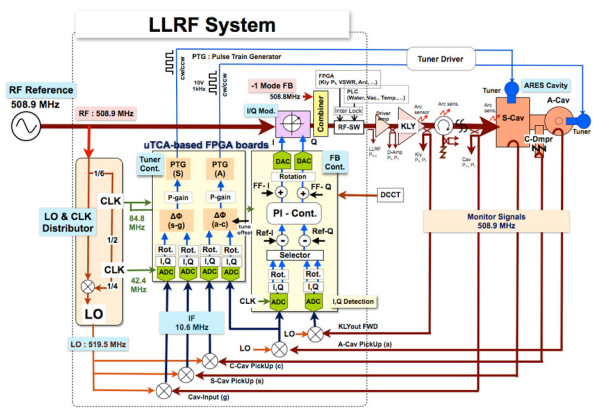


Figure 12: Block diagram of then new LLRF control system for the ARES cavity station.

ISBN: 978-3-95450-216-5 doi:10.18429/JACoW-eeFACT2018-WEYAA03

production model of the new LLRF system for the SuperKEKB. A block diagram of an ARES cavity driving system is shown Fig. 12. The principal functions of this system are performed by five FPGA boards which work on MicroTCA platform as advanced mezzanine cards [19]: Vc-FB controller (FBCNT), cavity-tuner controller (TNRCNT), inter-lock handler (INTLCNT), RF-level detector for the interlock and arc-discharge photo-signal detector. As shown in Fig.12, the new LLRF control system handles I/Q components of controlling signals in the FPGAs. For slow interlocks (e.g. vacuum, cooling water) and sequence control, a PLC is utilized. EPICS-IOC on Linux -OS is embedded in each of the FPGA boards and the PLC [20].

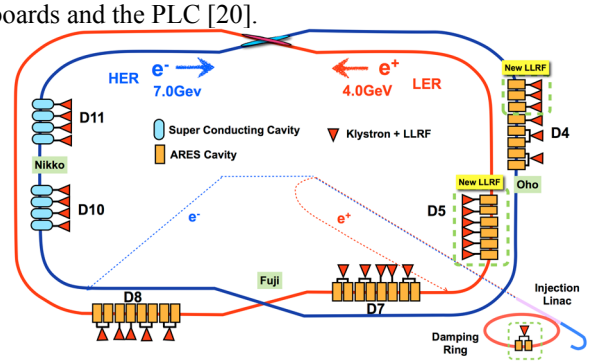


Figure 13: RF system layout for SuperKEKB Phase-1 and Phase-2. Nine LLRF stations were replaced with the new LLRF control system. The new LLRF control system for the damping ring was also newly installed.

In the present state, as shown in Fig. 13, the new digital LLRF control system is applied to 9 stations of ARES at Oho D4 and D5 in the main ring for SuperKEKB Phase-1 operation. Furthermore, the damping ring, which was constructed to reduce emittacne of positron beam, is also operated with the new LLRF control system. All of new systems successfully worked well without serious problem in Phase-1 and Phase-2.

On the other hands, the other stations including SCC stations were still operated with existing (old analogue) LLRF control systems, which had been used in the KEKB operation. The digital LLRF control system for SCC will be developed in next year, and then the old ones will be replaced with new ones step by step to achieve the design current.

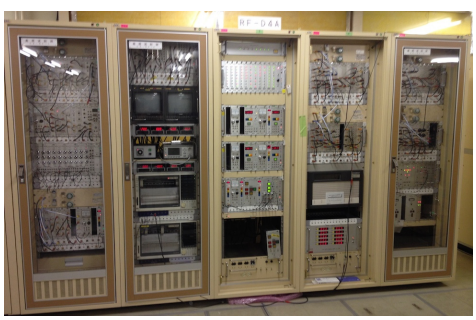

Figure 14: Old LLRF control system, which was used in KEKB operation, continues in use for SuperKEKB.Figure

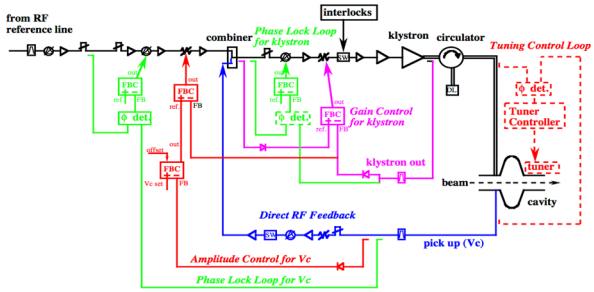


15: Block diagram of the old LLRF control system for the SCC RF station.

The existing analogue LLRF control systems are composed of combination of NIM standard analogue modules as shown in Fig. 14. Block diagram of the analogue system is shown in Fig. 15. It shows the cavity voltage (Vc amplitude and phase) regulation loop and the cavity tuner control with mechanical tuner and piezo actuator. Direct feedback method is also used in order to suppress coherent beam oscillations. For the detail of the analogue LLRF control system, Ref. [2]. These old systems are controlled remotely via CAMAC system. In the Phase-1 and Phase-2 operation, all systems also soundly worked as well as operated in the KEKB operation, although many old defective modules were replaced with spares in maintenance works.

### *Coupled Bunch Instabilities due to Acc. Mode*

Excitation of longitudinal coupled bunch instabilities (LCBI) caused by an accelerating mode is one of the serious problems for high-current beam storage. In the KEKB operation, so called $\mu$=-1 mode of LCBI had been excited by accelerating cavities. Accordingly, as shown in Fig. 16, a feedback system of LCBI damper had been applied for suppression of the $\mu$=-1 mode in KEKB operation [21].

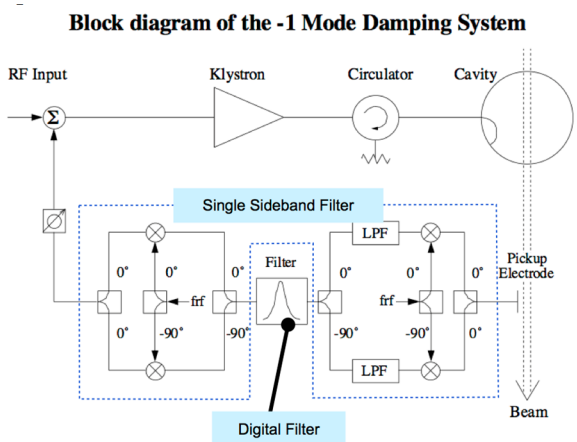


Figure 16: Block diagram of the $\mu$=-1 mode damping system, which had been used in KEKB operation. The $\mu$=-1 mode digital feedback selectively reduces impedance at the driving frequency.

For SuperKEKB upgrade which is aiming at 40-times higher luminosity than that of KEKB, LCBI will become more serious problem. Figure 17 shows estimation of the

ISBN: 978-3-95450-216-5 doi:10.18429/JACoW-eeFACT2018-WEYAA03



growth rates of LCBI due to the accelerating mode plotted as function of the stored beam current for SuperKEKB HER (upper side) and LER (lower side). The black horizontal line shows the radiation-damping rate, which corresponds to threshold for the instabilities. At the design current, optimum (de-)tuning $\Delta f$ for SC cavity will be approximately -44 kHz to compensate reactive component due to heavy beam loading, while the revolution frequency is about 100 kHz.

The dashed line in the Fig. 17 indicates the grow rate for case that one cavity is parked with -150-kHz detuning due to some troubles.

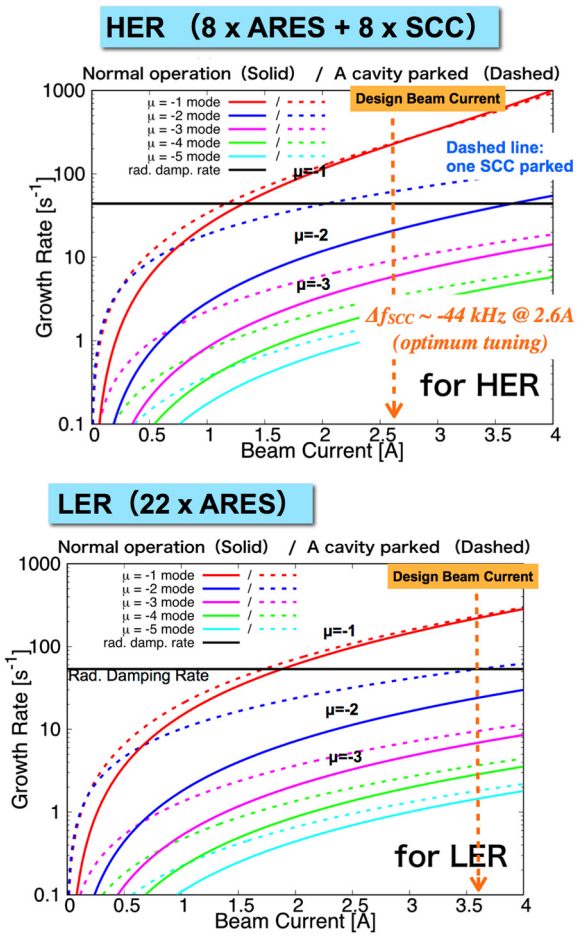


Figure 17: Estimation of the growth rates of LCBI due to the accelerating mode plotted as function of the stored beam current for SuperKEKB HER (upper side) and LER (lower side). Dashed line indicates the case of one cavity parked.

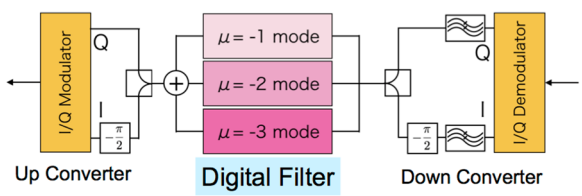


Figure 18: The new LCBI damper with new digital band-pass filters. The three LCBI modes can be treated in parallel, and the feedback parameters can be fine-tuned via EPICS, independently for each mode.

From the estimation of Fig. 17, it is predicted that $\mu$=-2 and -3 modes, in addition of $\mu$=-1 mode, will be excited for achievement of the design currents of SuperKEKB. Therefore, a new LCBI damper system, which can suppress these modes, was developed for SuperKEKB [22]. The digital band-pass filter of the new damper can filter the LCBI modes in parallel for feedback to damp LCBIs as shown in Fig. 18, and its feedback parameters (phase, gain, mode frequency and etc.) can be fine-tuned via EPICS, independently for each mode. Independent phase tuning for the respective mode is very essential in our RF system, since the klystron bandwidth is not enough broad (~130 kHz) in comparison to the revolution frequency.

The performance of the new LCBI damper was demonstrated at 620-mA beam current in the Phase-2 operation. The result is shown in Fig. 19. We excite the $\mu$=-2 mode instability on purpose by detuning a SC cavity manually in HER (upper side of Fig. 19), and then the $\mu$=-2 mode could be successfully suppressed by applying the new LCBI damper to the LLRF feedback control for ARES cavity station (lower side of Fig. 19).

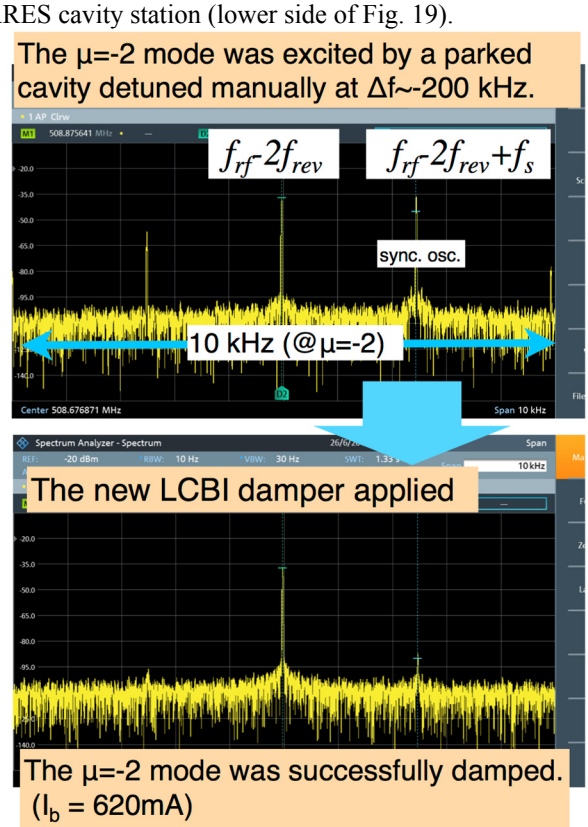


Figure 19: Demonstration of the new LCBI damper at 620-mA beam current in the Phase-2 operation. The $\mu$=-2 mode was excited by a parked SC cavity with manual detuning (upper side). Applying the new damper feedback suppressed the LCBI mode successfully (lower side).

## SUMMARY

### *Against Large HOM Load*

By development of a new calculation method with CST particle studio, the distribution of HOM load in the cavity module can be estimated. Calculated results showed the

ISBN: 978-3-95450-216-5 doi:10.18429/JACoW-eeFACT2018-WEYAA03

loads of SBP and LBP ferrite dampers are not large. However the large HOM power is emitted out toward the next cavity. To reduce the emission power, additional SiC damper was studied. The simulation showed that the SiC damper can absorb enough emission power and the SiC of 240 mm length is suitable for our SCC module. The prototype SiC damper has been installed and successfully reduced the emission power to the downstream cavity.

### *Recovering Degraded Cavity*

We have developed a horizontal HPR system with ultra-pure water. This system allows us to apply HPR to the cavity without disassembling the cryomodule. It means that many risks of re-assemble can be avoided. The HHPR was applied to three degraded cavities. The Qo values were successfully recovered in all cavities. Two cavity modules have been installed to the SuperKEKB ring. Another one is reserved as a spare cavity module. The technique of HHPR to recover the cavity performance has been established. We will apply HHPR to other cavities when they significantly degrade during the SuperKEKB operation.

### *LLRF Control Issues*

A new low-level RF (LLRF) control system, which is based on recent digital architecture, was developed for the SuperKEKB upgrade in order to make highly accurate and flexible Vc contro. It was applied to nine klystron stations among about 30 stations for the normal conducting cavity called ARES in the main ring of SuperKEKB, and it worked successfully in the Phase-1 and Phase-2 operation. The digital LLRF control system for SC cavities will be developed in next year, and then old LLRF systems will be replaced with new ones step by step for achievement the design currents of SuperKEKB.

A flexible and fine-tuneable LCBI damper was newly developed for SuperKEKB. The new LBCI damper can suppress the $\mu$=-1, 2 and 3 modes cased by the accelerating mode in parallel, and the feedback parameters (phase, gain and mode frequency) can be controlled remotely in high resolution, independently for respective mode. The performance of the new LCBI damper was demonstrated in the Phase-2 operation. It also worked as expected, and it could suppress LCBIs successfully.

## REFERENCES


[1] T. Abe *et al*., Prog. Theor. Exp. Phys. (2013) 03A001.

[2] K. Akai *et al*., "RF systems for the KEK B-Factory," *Nucl. Instrum. Meth. A* 499, 45–65 (2003)

[3] T. Abe, *et al*., "Performance and operation results of the RF systems at the KEK B-Factory", *Prog. Theor. Exp. Phys.* 2013, 03A006 (2013)

[4] T. Furuya, *et al*., "Superconducting Accelerating Cavity for KEK B-factory," *Proceedings of SRF1995*, CEA-Saclay, France, 1995, p. 729 (1995).

[5] S. Mitsunobu, *et al*., "High Power Test of the Input Coupler for KEKB SC Cavity," *Proceedings of SRF1995*, CEA-Saclay, France, 1995, p. 735 (1995).

[6] Y. Yamazaki and T. Kageyama, "A Three-Cavity System which Suppresses the Coupled-Bunch Instability Associated with the Accelerating Mode," *Part. Accel.*, 44, 107 (1994)

[7] T. Kageyama *et al*., "The ARES cavity for KEKB," *Conf. Proc. of APAC98*, pp. 773-775 (1998)

[8] K. Akai *et al*., "Design Progress and Construction Status of SuperKEKB," *IPAC2012*, New Orleans, May 2012, TUPPR006, p. 1822 (2012); http://accelconf.web.cern.ch/accelconf/IPAC2012/papers/tuppr006.pdf

[9] Y.Ohnishi, "Report on SuperKEKB Phase 2 Commisioning", *Proceedings of IPAC2018*, Vancouver, BC, Canada, 2018, MOXGB1, pp. 1-5.

[10] A. Morita, "Status of SuperKEKB phase-2 commissioning", *ICHEP2018,* 877; https://indico.cern.ch/event/686555/contributions/2962552/

[11] K. Akai, "SuperKEKB/Belle II Status", *ICHEP2018*, 1072; https://indico.cern.ch/event/686555/contributions/3028068/

[12] Y. Morita *et al.*, "KEKB Superconducting Accelerating Cavities and Beam Studies for Super-KEKB", Proc. of IPAC'10, Kyoto, Japan, 2010, p.1536-1538.

[13] T. Tajima, "Development of Higher-Order-Mode (HOM) Absorbers for KEKB Superconducting Cavities," KEK Report 2000-10 (2000).

[14] M. Nishiwaki *et al.*, "Developments of HOM Dampers for SuperKEKB Superconducting Cavity," *SRF2013*, Paris, Sept. 2013, TUP061, p. 1052 (2013); http://ipnweb.in2p3.fr/srf2013/papers/thp061.pdf

[15] M. Nishiwaki *et al.*, "Developments of SiC Damper for SuperKEKB Superconducting Cavity", *Proc. of SRF2015*, Whistler, BC, Canada, 2015, p.1289-1292.

[16] Y. Morita et al., "Horizontal High Pressure Water Rinsing for Performance Recovery," *SRF2013*, Paris, Sept. 2013, TUP051, p. 521 (2013); http://ipnweb.in2p3.fr/srf2013/papers/tup051.pdf

[17] Y. Kijima, *et al*., "Conditioning of Input Couplers for KEKB Superconducting Cavities," *Proc. of the 10th Workshop on RF Superconductivity, KEK/JAERI*, Tsukuba, 6 – 11 September 2001, pp. 565-569 (2001).

[18] T. Kobayashi *et al.*, "Development and Construction Status of New LLRF Control System for SuperKEKB", *in Proc. of IPAC'14*, paper WEPME071, pp. 2444-2446.

[19] M. Ryoshi et al., "LLRF Board in Micro-TCA Platform," *Proc. of the 7th Annual Meeting of Particle Acc. Society of Japan*, p. 668 (2010).

[20] J. Odagiri *et al.*, "Fully Embedded EPICS-Based Control of Low Level RF System for SuperKEKB," *Proc. of IPAC'10*, p. 2686 (2010).

[21] S. Yoshimoto *et al*., "The -1 Mode Damping System for KEKB", *Proc. of The 14th Symposium on Accelerator Science and Technology*, 1P072 (2003)

[22] K. Hirosawa *et al*., "A New Damper for Coupled-Bunch Instabilities caused by the accelerating mode at SuperKEKB", *Proc. of LLRF2017*, arXiv:1803.10886; https://arxiv.org/pdf/1803.10886.pdf